

## CzeV404 Herculis - an eclipsing dwarf nova in the period gap during its July 2014 superoutburst

K. Bąkowska<sup>1</sup>, A. Olech<sup>1</sup>, R. Pospieszynski,  
F. Martinelli<sup>2</sup> & A. Marciniak<sup>3</sup>

<sup>1</sup> Nicolaus Copernicus Astronomical Center, Polish Academy of Sciences,  
ul. Bartycka 18, 00-716 Warszawa, Poland

<sup>2</sup> Lajatico Astronomical Centre, Loc i Fornelli N°9, Orciatice Lajatico, Pisa, Italy

<sup>3</sup> Astronomical Observatory Institute, Faculty of Physics, A.Mickiewicz University,  
ul. Słoneczna 36, 60-286 Poznań, Poland  
e-mail: bakowska@camk.edu.pl

### Abstract

Results of the CCD observations of CzeV404 Her are displayed. During the season of June-August 2014 we detected one outburst and one superoutburst of the star. Clear superhumps with the period of  $P_{sh} = 0.10472(2)$  days were observed. The superhump period was decreasing with a high value of  $\dot{P} = -2.43(8) \times 10^{-4}$ . For 17 eclipses, we calculated an orbital period with the value of  $P_{orb} = 0.0980165(5)$  days which indicates that CzeV404 Her belongs to period gap objects and it is the longest orbital period eclipsing SU UMa star. Based on superhump and orbital period determinations, the period excess  $\varepsilon = 6.8\% \pm 0.02\%$  and the mass ratio  $q \approx 0.32$  of the system were obtained.

**Key words:** Stars: individual: CzeV404 Her - binaries: close - novae, cataclysmic variables

## 1 Introduction

Cataclysmic variables (CVs) are interacting binary stars which contain a white dwarf (the primary) and an orbiting companion, usually a main-sequence star (the secondary or the donor). The material is accreted by the primary through the inner Lagrangian point from the Roche-lobe filling secondary. In non-magnetic CVs an accretion disk is formed around the white dwarf. The region where the matter collides with the edge of the disk is known as the hot spot (Warner 1995).

Dwarf novae (DNs) of a SU-UMa type are one of the subclasses of CVs. The characteristic feature of SU-UMa stars is short orbital period (below 2.5 h). In their light curves one can observe eruptions classified as outbursts or superoutbursts. Outbursts to superoutbursts occurrence ratio is ten to one. During superoutbursts SU UMa stars are about one magnitude brighter and, in the light curves, there are periodic light oscillations called superhumps. A superhump period is a few percent longer than the orbital period (more in Hellier 2001).

The period gap (from 2 to 3 hours) is an orbital period range where there is a significant dearth of active CVs. The standard evolution model assumes that around the  $P_{orb} \approx 3$  hours the donor becomes fully convective and the magnetic braking, which is responsible for the angular momentum loss, is

abruptly shut off. At that point CV systems evolve towards shorter periods as detached binaries. When the orbital period decreases to about 2 hours the mass transfer restarts. The angular momentum loss is caused by the emission of gravitational radiation (Paczynski 1981) and CVs reappear as active systems below the period gap (for a review Knigge et al. 2011).

Up to now the variable star CzeV404 Her was analyzed only once; Cagaš and Cagaš (2014) presented results of two observing campaigns of CzeV404 Her spanning the period from June to September 2012 and June to August 2012. During that time one superoutburst in August 2012 and a several outbursts during the 2013 observation season were detected. Based on their calculations, CzeV404 Her is an eclipsing cataclismic variable of a SU UMa type.

Light curves of eclipsing dwarf novae are a reliable diagnostic tool for the theoretical interpretation of superoutburst and superhump mechanisms (check Smak 2013a, 2013b, Bąkowska and Olech 2014b), hence our motivation for the new observing campaign of CzeV404 Her.

The structure of the paper is as follow: section 2 contains the description of observation runs, data reduction and global photometric behaviour of CzeV404 Her. In section 3 we present the periodicity of the detected superhumps and eclipses. Section 4 is a discussion chapter and the last section displays summary of our results.

## 2 Observations

Observations of CzeV404 Her reported in this work were obtained during 15 nights from 2014 June 18 to July 22 at the Borowiec station of Poznań Astronomical Observatory located in Poland and during 3 nights from 2014 July 27 to August 1 in Pisa in Italy. During this time span we detected one outburst (monitored during 3 nights) and one superoutburst (observed during 9 nights).

Most of our observations (first 15 nights) were carried out at the Borowiec Station. We used a 40 cm, F/4.5 Newton reflector, equipped with a ST-7 CCD camera providing a  $8.0' \times 12.0'$  field of view.

Due to unfavorable weather conditions in the last 3 nights of our campaign, data collection was performed in Italy. For this set of observations a Newton reflector with a 12" diameter, equipped with a KAF402 CCD camera was used.

In order to obtain the shortest possible exposure times all observations of the CzeV404 Her were made in the "white light" (clear filter). The exposure times ranged from 60 to 240 seconds depending on the weather conditions and the brightness of the object.

In total, we gathered 54.5 hours and obtained 2193 exposures of CzeV404 Her during 18 nights. Table 1 presents a full journal of our CCD observations.

### 2.1 Data Reduction

We determined relative unfiltered magnitudes of CzeV404 Her by taking the difference between the magnitude of the variable and the mean magnitude of the three comparison stars. In Fig. 1 the map of a region is displayed with the variable star marked as V1 and the comparison stars as C1, C2 and C3, respectively. The equatorial coordinates and the brightness of comparison star C3 (RA= $18^h 30^m 22^s .239$ , Dec= $+12^{\circ} 32' 26'' .17$ , 12.63 mag in  $V_T$  filter) are taken from the Tycho-2 Catalogue (Hog et al. 2000).

We performed all of the data reductions using the IRAF<sup>1</sup> package. Profile photometry was obtained with DAOPHOTII (Stetson 1987).

---

<sup>1</sup>IRAF is distributed by the National Optical Astronomy Observatory, which is operated by the Association of Universities for Research in Astronomy, Inc., under a cooperative agreement with the National Science Foundation.

Table 1: The journal of our CCD observations of CzeV404 Her.

Date	Time of start 2456000+ [HJD]	Length of run [h]	Number of frames	Telescope	Observer
2014 June 18	827.37813	2.38	33	Borowiec	K. Bąkowska
2014 June 23	832.38466	3.78	147	Borowiec	K. Bąkowska
2014 June 26	835.41737	2.33	67	Borowiec	R. Pospieszynski
2014 July 01	840.43256	1.25	73	Borowiec	K. Bąkowska
2014 July 02	841.36717	3.21	180	Borowiec	R. Pospieszynski
2014 July 03	842.36747	1.77	102	Borowiec	R. Pospieszynski
2014 July 04	843.37035	1.31	50	Borowiec	R. Pospieszynski
2014 July 06	845.36662	2.31	90	Borowiec	R. Pospieszynski
2014 July 15	854.42864	3.23	124	Borowiec	K. Bąkowska
2014 July 16	855.38603	1.78	103	Borowiec	K. Bąkowska
2014 July 17	856.34946	4.63	230	Borowiec	R. Pospieszynski
2014 July 18	857.37171	3.43	199	Borowiec	K. Bąkowska
2014 July 19	858.34480	5.29	196	Borowiec	R. Pospieszynski
2014 July 20	859.37679	4.32	154	Borowiec	A. Marciniak
2014 July 22	861.36142	4.78	180	Borowiec	A. Marciniak
2014 July 27	866.40934	4.60	140	Pisa	F. Martinelli
2014 July 31	870.36370	1.83	51	Pisa	F. Martinelli
2014 August 1	871.34353	2.31	74	Pisa	F. Martinelli

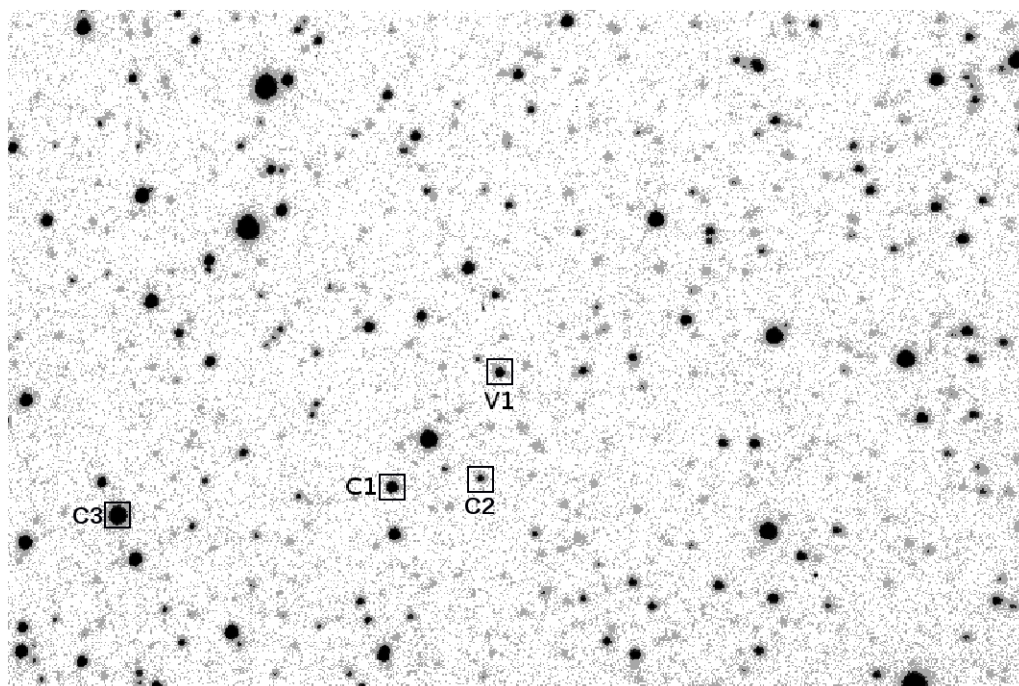


Figure 1: Finding chart of CzeV404 Her. The variable is marked as V1. Positions of the three comparison stars C1, C2 and C3 are also shown. The field of view is about  $8.0' \times 12.0'$ . North is up, east is left.

The accuracy of our measurements varied between 0.006 and 0.085 mag for observations from Poland, 0.006 and 0.045 mag for the data set from Italy, depending on the atmospheric conditions and brightness of the variable. The median value of the photometry errors was 0.010 mag and 0.013 mag for Borowiec and Pisa observations, respectively.

## 2.2 Light curves

From now on we use only a day number HJD-2456000 [d] to refer to our observations. In Fig. 2 one can see the global light curve of CzeV404 Her from 2014 June 18 to August 1.

In the beginning of our observations (HJD 827 – 835) CzeV404 Her was in quiescence with a brightness varying between  $V_T \approx 16.6$  and  $V_T \approx 17.0$  mag. Later (HJD 840 – 842), we caught the variable during the outburst with the maximum brightness of  $V_T \approx 15.5$  mag. Due to lack of observations between HJD 836 – 839, caused by weather conditions, we can only say that the outburst lasted at least 3 nights and the amplitude was not lower than  $A_o \approx 1.5$  mag. Based on these estimate, it is highly probable that we observed almost the whole outburst. On HJD 854 the superoutburst started and lasted for 17 nights. During the superoutburst the brightness of CzeV404 Her reached  $V_T \approx 15.0$  mag at maximum and decreased to  $V_T \approx 17.2$  mag at minimum, resulting in the amplitude of  $A_s \approx 2.2$  mag.

In Fig.3 we present the individual light curves from four nights HJD 856 – 861 of the variable during its July 2014 superoutburst. Short-term modulations known as superhumps are visible during all of the four displayed nights.

## 3 Superhumps and Orbital Periods

### 3.1 ANOVA Power Spectrum

We removed the long term trend from the observations of CzeV404 Her which covered the July superoutburst and then analyzed them with ANOVA statistics (Schwarzenberg-Czerny 1996). Fig. 4 shows the resulting periodogram where the two highest signals are marked by open black squares. The most prominent peak was found at a frequency of  $f_1 = 10.200 \pm 0.020$  c/d, which corresponds to the period of  $P_{orb1} = 0.09804(19)$  days ( $141.18 \pm 0.28$  min) and we interpret it as an orbital signal.

The second peak was observed at a frequency of  $f_2 = 9.600 \pm 0.055$  c/d, which is equal to the period of  $P_{sh1} = 0.10417(60)$  days ( $150.05 \pm 0.86$  min). This signal is a manifestation of superhumps.

We tried to remove eclipses by hand from original light curves to obtain frequency pattern only for superhump periodicity. However, the resulting periodogram still displayed both frequencies from orbital and superhumps signals. Also, after the classical prewhitening procedure the result remained the same. We were not able to get the periodogram exclusively for superhump signal because of the changing amplitude of superhump wave, flickering and short observing runs during July nights.

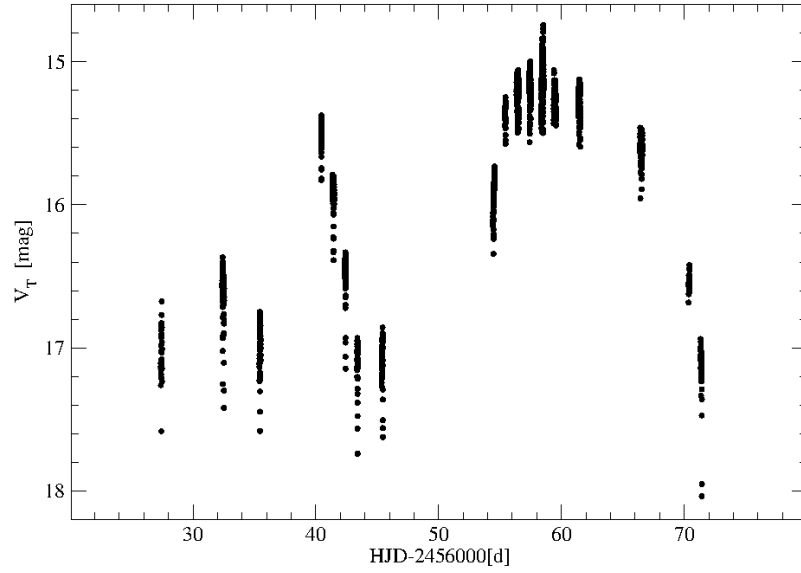


Figure 2: Global photometric behaviour of CzeV404 Her during our observational campaign in June-August 2014.

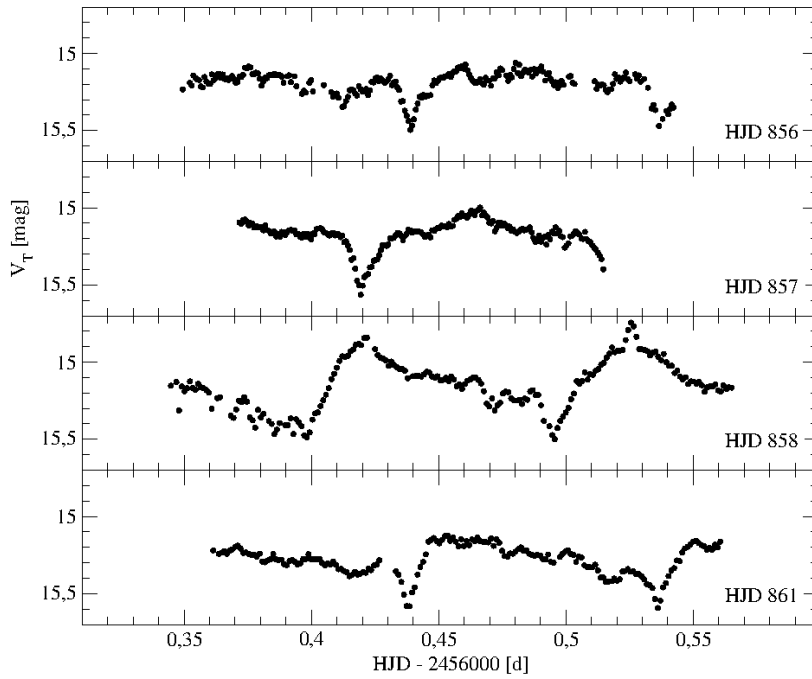


Figure 3: Light curves of CzeV404 Her during its superoutburst in July 2014. A fraction of HJD is presented on the  $x$ -axis. Additionally, HJD–2456000 [d] is given on the right side of each panel.

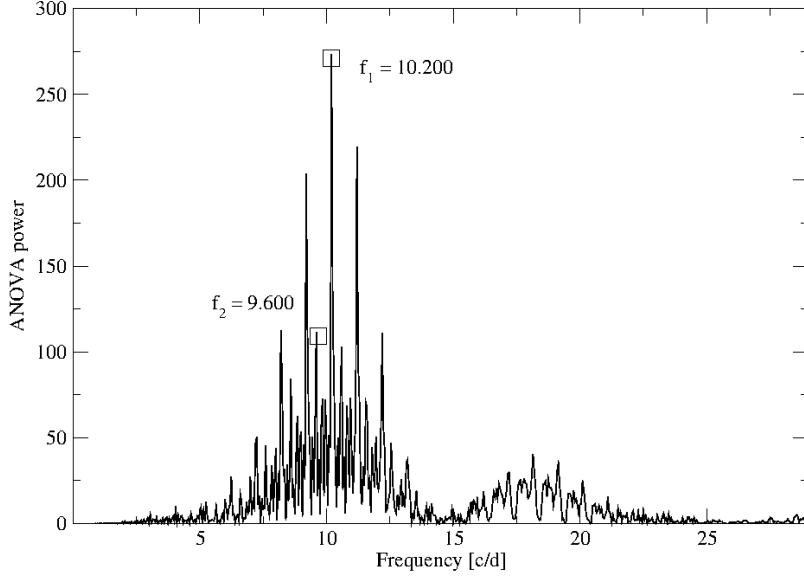


Figure 4: ANOVA power spectrum of the light curves of CzeV404 Her during its July 2014 superoutburst. Two highest peaks  $f_1$  and  $f_2$ , marked by open squares, correspond to the orbital and the superhump frequencies, respectively.

### 3.2 $O - C$ Diagram for Superhumps

To calculate the period of light modulations during the superoutburst we constructed the  $O - C$  diagram for the times of superhumps maxima. In total, we determined nine peaks of maxima, which are listed in Table 2 together with their errors, cycle numbers  $E$  and  $O - C$  values.

The least squares linear fit to the data presented in Table 2 allowed to obtain the following ephemeris:

$$\text{HJD}_{\max} = 2456856.4286(5) + 0.10472(2) \times E \quad (1)$$

which indicates that the value of the superhump period is  $P_{sh2} = 0.10472(2)$  days ( $150.80 \pm 0.03$  min).

In Fig. 5 we display, as black filled diamonds, the  $O - C$  values corresponding to the ephemeris (1).

The decreasing trend of the superhump period shown in Fig.5 was confirmed by calculations of the second-order polynomial fit to the moment of maxima. The following ephemeris was estimated:

$$\text{HJD}_{\max} = 2456856.4055(9) + 0.10618(5) \times E - 1.29(4) \times 10^{-5} \times E^2 \quad (2)$$

In Fig. 5 the solid line corresponds to the ephemeris (2).

After this investigation, we conclude that the period of superhumps was not stable during the July 2014 superoutburst of CzeV404 Her and it can be described by a decreasing trend with a rate of

$\dot{P} = -2.43(8) \times 10^{-4}$ . Due to the fact that the superhump period from ANOVA analysis has 10 times higher error order of magnitude than the value obtained from  $O - C$  analysis as the final superhump period we establish the value of  $P_{sh2}$  given in ephemeris (1).

Table 2: Times of superhumps maxima in the light curves of CzeV404 Her during its July 2014 superoutburst.

$E$	HJD <sub>max</sub> - 2456000	Error	$O - C$ [cycles]
0	856.3774	0.0020	-0.4885
1	856.4911	0.0020	-0.4026
10	857.4666	0.0015	-0.0855
19	858.4215	0.0005	0.0349
20	858.5260	0.0005	0.0330
48	861.4652	0.0010	0.1055
95	866.3655	0.0020	-0.0912
97	866.5715	0.0030	-0.1237
134	870.4270	0.0030	-0.2994

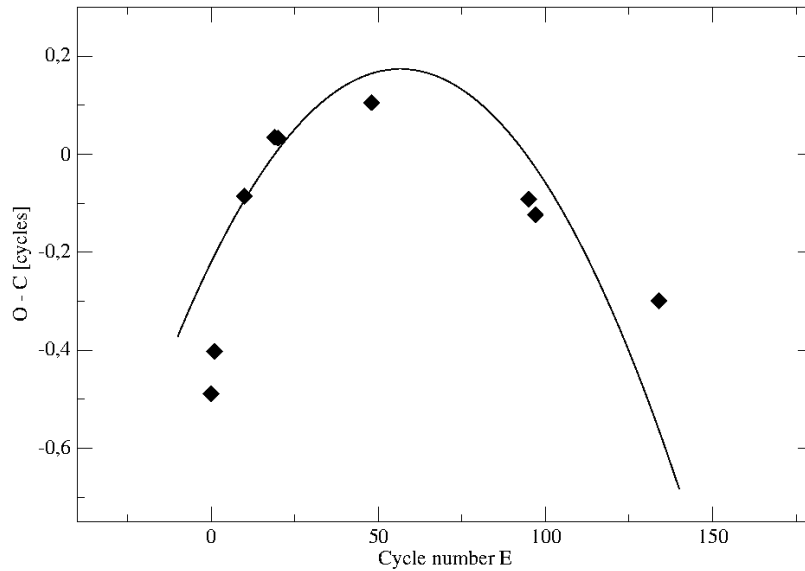


Figure 5: The  $O - C$  diagram for the superhumps maxima of CzeV404 Her observed during its superoutburst in July 20. The solid line corresponds to the fit presented in Eq.(2).

### 3.3 $O - C$ Diagram for Eclipses

We obtained the value of the orbital period by constructing the  $O - C$  diagram for the moments of the minima. In total, we used the timings of 17 eclipses from the June-August 2014 observing season and the following ephemeris of the minima was derived:

$$\text{HJD}_{\min} = 2456827.4252(1) + 0.0980165(5) \times E \quad (3)$$

which equals the orbital period of  $P_{orb2} = 0.0980165(5)$  days ( $141.1438 \pm 0.0007$  min).

In Table 3 we present the timings of eclipses with errors, cycle numbers  $E$  and  $O - C$  values. The resulting  $O - C$  diagram for the moments of minima is shown in Fig. 6.

Between the superhump and orbital periods there is a relation introduced by Osaki (1985):

$$\frac{1}{P_{sh}} = \frac{1}{P_{orb}} - \frac{1}{P_{beat}}, \quad (4)$$

and we used Eq.(4) and the orbital  $P_{orb2}$  and superhump  $P_{sh2}$  periods to calculate the beat period of  $P_{beat} = 1.53 \pm 0.02$  days.

In Fig. 6, during the superoutburst, values of the  $O - C$  cycles from  $E = 286$  to  $E = 449$  were more scattered than in quiescence (from  $E = 0$  to  $E = 184$ ). It is possible the beat period manifestation (the same as in HT Cas during Nov 2010 superoutburst, Fig. 3 Bąkowska et al. 2014a). However, we do not have sufficient amount of data points of the minima of eclipses to postulate that.

To obtain the best possible value of the orbital period we combined our 17 timings of eclipses from 2014 and 16 from the 2012-2013 observations presented by Cagaš and Cagaš (2014). Based on this, we calculated the following ephemeris of the minima:

$$\text{HJD}_{\min} = 2456827.42359(5) + 0.09802201(2) \times E \quad (5)$$

and this corresponds to the orbital period of  $P_{orb3} = 0.09802201(2)$  days ( $141.15169 \pm 0.00003$  min). In Fig. 7 we show the resulting  $O - C$  diagram for the moments of eclipses for 2012-2014 time span.

## 4 Discussion

Knowing the orbital and superhump periods we can draw conclusions about the evolution of CzeV404 Her. In the diagram  $P_{orb}$  versus  $\varepsilon$  presented in Fig. 8 we display SU UMa stars, period bouncers and nova-like variables. The period excess was calculated as:

$$\varepsilon = \frac{\Delta P}{P_{orb}} = \frac{P_{sh} - P_{orb}}{P_{orb}}. \quad (6)$$

and for CzeV404 Her we obtained a value of  $\varepsilon = 6.8\% \pm 0.02\%$ .



Table 3: Times of minima in the light curves of CzeV404 Her observed in the period of June-July 2014.

$E$	$\text{HJD}_{\min} - 2456000$	Error	$O - C$ [cycles]
0	827.4253	0.0005	0.0009
51	832.4242	0.0002	0.0015
52	832.5219	0.0002	-0.0017
82	835.4628	0.0004	0.0024
133	840.4615	0.0005	0.0010
143	841.4417	0.0002	0.0013
153	842.4216	0.0003	-0.0014
163	843.4030	0.0005	0.0112
184	845.4598	0.0003	-0.0046
286	855.4583	0.0004	0.0038
296	856.4388	0.0003	0.0072
297	856.5370	0.0003	0.0091
306	857.4194	0.0002	0.0116
317	858.4956	0.0001	-0.0065
347	861.4380	0.0003	0.0101
348	861.5361	0.0003	0.0117
449	871.4362	0.0005	0.0090

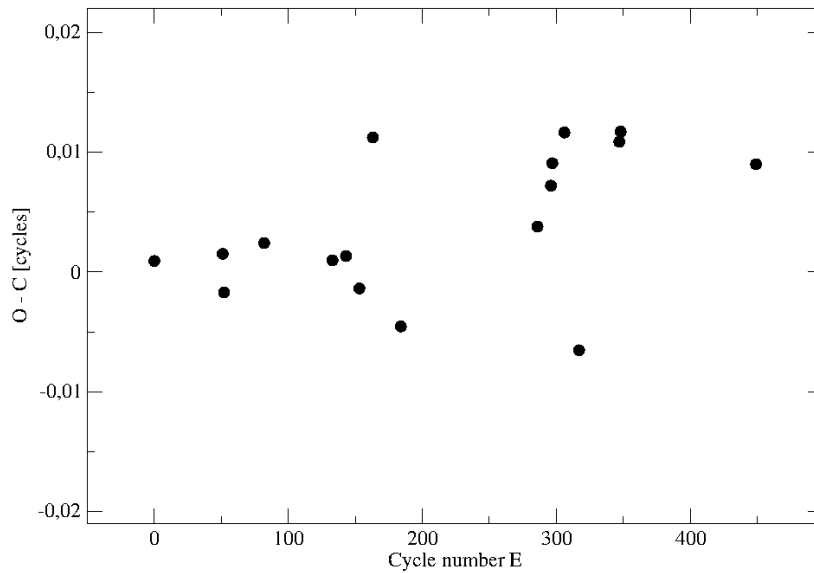


Figure 6: The  $O - C$  diagram for the moments of eclipses observed in CzeV404 Her during the June-August 2014 campaign.

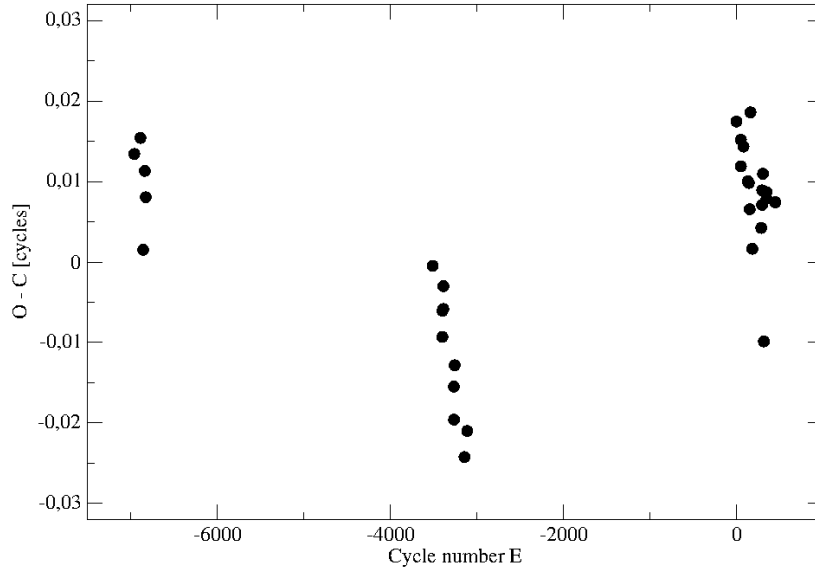


Figure 7: The  $O - C$  diagram for the moments of minima was based on our data set from 2014 and the data from 2012-2013 provided by Cagaš and Cagaš (2014).

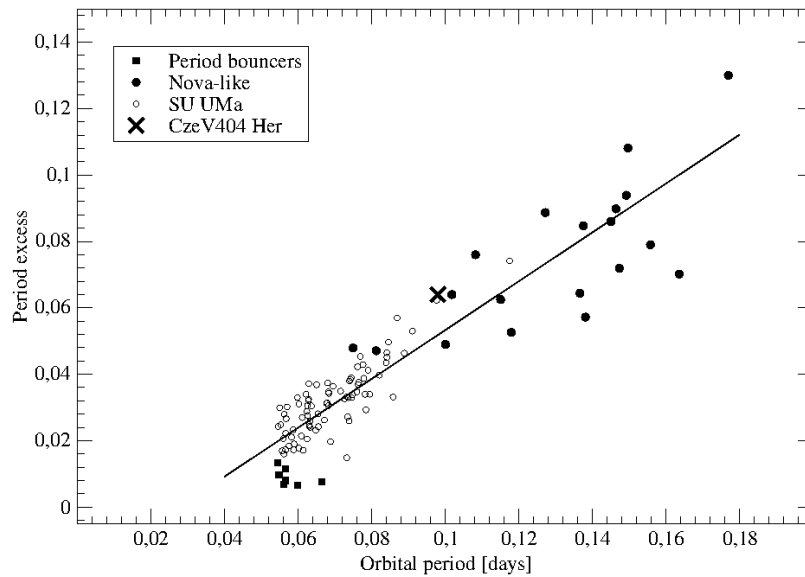


Figure 8: The relation between the period excess and the orbital period for several subclasses of CVs. CzeV404 Her is marked by a big, black X-mark. By open circles we plotted SU UMa type stars. Nova-like variables are illustrated by black dots. The period bouncer candidates are represented by black squares (figure taken from Olech et al. 2011).

The mass ratio of the binary  $q = M_2/M_1$  can be obtained from the empirical formula introduced by Patterson (1998):

$$\varepsilon = \frac{0.23q}{1 + 0.27q}. \quad (7)$$

This results with the  $q \approx 0.32$  for CzeV404 Her. The tidal instability (Whitehurst 1988) of the disk starts to work effectively for binaries with a mass ratio  $q$  below 0.25. This assumption was used by Osaki (1989) in the TTI (thermal-tidal instability) model to explain the phenomenon of superoutbursts and superhumps. That is why such a high value of  $q$  in CzeV404 Her poses a serious problem for the superhump mechanism.

The detection of active DNs in the period gap, i.e. MN Dra (Nogami et al. 2003), NY Ser (Pavlenko et al. 2010, 2014), SDSS J162520.29+120308.7 (Olech et al. 2011), OGLE-BLG-DN-001 (Poleski et al. 2011) is another issue in the evolution of CVs. There are two mechanisms which are thought to drive the orbital angular momentum loss. First one is the magnetic wind breaking which is greatly reduced around orbital period  $P_{orb} \approx 3$  hours when the secondary becomes fully convective (Verbunt and Zwaan 1981) and the donor detaches from its Roche-lobe. Between the 2–3 hour orbital period range, known as the orbital period gap, the number of CVs found is very low (see Gänsicke et al. 2009). At around  $P_{orb} \approx 2$  hours (Howell et al. 2001) the mass transfer is resumed because the secondary reestablished the Roche lobe contact. Further evolution of CVs is driven mainly by the second mechanism of the orbital angular momentum loss known as the gravitational radiation (Paczynski 1981). SU UMa stars located in period gap and having Roche lobe filling secondaries should be driven by gravitational wave radiation. At this orbital period ( $\sim 2.5$  H) both the angular momentum loss as well as the mass transfer should be low and according to the TTI model these objects should be characterized by low activity. It is certainly not the case in such systems as CzeV404 Her or MN Dra.

The first suggestion that superhump period in majority of SU UMa stars changes with the common pattern appeared in Olech et al. (2003, 2004). Since 2009, Kato et al. (2009, 2010, 2012, 2013, 2014a, 2014b) published extensive surveys concerning superhump period changes observed in SU UMa stars. According to these works the evolution of superhump period can be divided into three parts: stage A with a stable and longer period, stage B characterized by a positive period derivative and the last stage C with a shorter and stable period. Several active DNs in the period gap, i.e. SDSS J170213 (Kato et al. 2013), CSS J203937, V444 Peg, MASTER J212624 (Kato et al. 2014a) and MN Dra (Kato et al. 2014b) were presented in surveys supervised by the Japanese team and a part of them followed this scenario. However, some of the long period SU UMa stars seem to show only a decreasing superhump period across the entire superoutburst (see for example SDSS J1556 and UV Per in Kato et al. 2009). CzeV404 Her seems to belong to the same group. Our observations cover the entire superoutburst and there is a clear and a rather constant superhump period decrease observed over the whole interval of 17 days.

It is worth noting that some of the CzeV404 Her system parameters are similar to MN Dra, respectively, i.e. orbital periods  $P_{orb} = 0.0998(2)$  days (Pavlenko et al. 2010) and  $P_{orb} = 0.0980165(5)$  days (this work), superhump periods  $P_{sh} = 0.105040(66)$  days (Kato et al. 2014b) and  $P_{sh} = 0.10472(2)$  days (this work), the large period variations  $\dot{P} = -1.48(95) \times 10^{-4}$  (Kato et al. 2014b) and  $\dot{P} = -2.43(8) \times 10^{-4}$  (this work), and the mass ratio  $q \approx 0.29$  (Kato et al. 2014b) and  $q \approx 0.32$  (this work). That is why both of these active DNs from the period gap deserve more observations for further analysis of CV stars evolution.

## 5 Conclusions

We summarize the results of the summer 2014 campaign of CzeV404 Her:

- During the two and half months of observations from 2014 June 18 to August 1 we detected one outburst and one superoutburst in CzeV404 Her. The outburst lasted at least 3 nights and the amplitude was not fewer than  $A_o \approx 1.5$  mag. The June 2014 superoutburst had the amplitude of brightness  $A_s \approx 2.2$  mag and had a duration of 17 nights. Clear superhumps were detected during the superoutburst.
- ANOVA statistics (Schwarzenberg-Czerny 1996) was used to calculate the periodogram of CzeV404 Her. The most prominent peak was found at a frequency of  $f_1 = 10.200 \pm 0.020$  c/d, which corresponds to the orbital period of  $P_{orb1} = 0.09804(19)$  days ( $141.18 \pm 0.28$  min). The second peak was observed at a frequency of  $f_2 = 9.600 \pm 0.055$  c/d, which is equal to the superhump period of  $P_{sh1} = 0.10417(60)$  days ( $150.05 \pm 0.86$  min).
- Based on the maxima of superhumps we calculated the superhump period  $P_{sh2} = 0.10472(2)$  days ( $150.80 \pm 0.03$  min). The orbital period  $P_{orb2} = 0.0980165(5)$  days ( $141.1438 \pm 0.0007$  min) was obtained using 17 eclipses. Combining our data set and the moments of eclipses provided by Cagaš and Cagaš (2014) we found a more precise orbital period with the value of  $P_{orb3} = 0.09802201(2)$  days ( $141.15169 \pm 0.00003$  min).
- The superhump period was not stable during the July 2014 superoutburst of CzeV404 Her and it was decreasing with the high value of  $\dot{P} = -2.43(8) \times 10^{-4}$ .
- With the Stolz-Schoembs (1984) formula we derived period excess  $\varepsilon = 6.8\% \pm 0.02\%$  and on the diagram  $P_{orb}$  versus  $\varepsilon$  CzeV404 Her is located in the period gap objects.
- The mass ratio with the value of  $q \approx 0.32$  was obtained. Such a high value is a problem for the TTI model assuming  $q < 0.25$  for the superhump and the superoutburst mechanism.

There is no doubt that CzeV404 Her is a unique variable star. It belongs to about one dozen of SU UMa stars located in the period gap. Its orbital period is one of the longest among whole group of SU UMa variables. Additionally, it is longest period eclipsing SU UMa star known and its high mass ratio poses a serious challenge for the TTI model. Certainly, CzeV404 Her needs to be studied further. Both high speed photometry with 2-meter class telescope as well as spectroscopy with the world's largest telescopes would allow to precisely determine the basic parameters of the binary system.

**Acknowledgments.** We acknowledge generous allocation of Poznań Observatory 0.4-m telescope time. Also, we want to thank mgr A. Borowska for language corrections. Project was supported by Polish National Science Center grant awarded by decision DEC-2012/07/N/ST9/04172 for KB.

## References

- [1] Bąkowska K., Olech A., Rutkowski A., Koff R., de Miguel E. and Otulakowska-Hypka M., 2014a, *Contrib. Astron. Obs. Skalnaté Pleso*, 43, 325
- [2] Bąkowska K. and Olech A., 2014b, *Acta Astron.*, 64, 247

- [3] Cagaš P. and Cagaš P., 2014, *IBVS*, 6097, 1
- [4] Gänsicke B.T., Dillon M., Southworth J. et al., 2009, *MNRAS*, 397, 2170
- [5] Hellier C., 2001, *Cataclysmic Variable Stars*, Springer
- [6] Hog E., Fabricius C., Makarov V.V. et al., 2000, *A&A*, 355, L27
- [7] Howell S.B., Nelson L.A. and Rappaport S., 2001, *ApJ*, 550, 897
- [8] Knigge C., Baraffe I. and Patterson J., 2011, *ApJS*, 194, 28
- [9] Kato T., Imada A., Uemura M. et al., 2009, *PASJ*, 61, S395
- [10] Kato T., Maehara H., Uemura M. et al., 2010, *PASJ*, 62, 1525
- [11] Kato T., Maehara H., Miller I. et al., 2012, *PASJ*, 64, 21
- [12] Kato T., Hamsch F.-J., Maehara H. et al., 2013a, *PASJ*, 65, 23
- [13] Kato T., Hamsch F.-J., Maehara H. et al., 2014a, *PASJ*, 66, 30
- [14] Kato T., Dubovsky P.A., Kudzej I. et al., 2014b, *arXiv:1406.6428*,
- [15] Nogami D., Uemura M., Ishioka R. et al., 2003, *A&A*, 404, 1067
- [16] Olech A., Schwarzenberg-Czerny A., Kędzierski P., Złoczewski K., Mularczyk K., Wiśniewski M., 2003, *Acta Astron.*, 53, 175
- [17] Olech A., Cook L.M., Złoczewski K., Mularczyk K., Kędzierski P., Udalski A., Wiśniewski M., 2004, *Acta Astron.*, 54, 233
- [18] Olech A., de Miguel E., Otulakowska M. et al. 2011, *A&A*, 532, A64
- [19] Osaki Y., 1985, *A&A*, 144, 369
- [20] Osaki Y., 1989, *PASJ*, 41, 1005
- [21] Paczyński B., 1981, *Acta Astron.*, 31, 1
- [22] Patterson J., 1998, *PASP*, 110, 1132
- [23] Pavlenko E., Kato T., Andreev M. et al., 2010, *17th European White Dwarf Workshop AIP Conference Proceedings*, 1273, 320
- [24] Pavlenko E.P., Kato T., Amtonyuk O.I. et al., 2014, *arXiv:1408.4285*)
- [25] Poleski R., Udalski A., Skowron J. et al., 2011, *Acta Astron.*, 61, 123
- [26] Schwarzenberg-Czerny A., 1996, *ApJ*, 460, L107
- [27] Stolz B. and Schoembs R., 1984, *A&A*, 132, 187
- [28] Smak J., 2013a, *Acta Astron.*, 63, 109

- [29] Smak J., 2013b, *Acta Astron.*, 63, 369
- [30] Stetson P.B., 1987, *PASP*, 99, 191
- [31] Verbunt F. and Zwaan C., 1981, *A&A*, 100, L7
- [32] Warner B., 1995, *Cataclysmic Variable Stars*, Cambridge University Press
- [33] Whitehurst R., 1988, *MNRAS*, 232, 35